New Mechanism for Electron Emission from Planar Cold Cathodes: The Solid-State Field-Controlled Electron Emitter

Vu Thien Binh[1,*] and Ch. Adessi[2]

[1]*Laboratoire d'Emission Electronique, DPM-CNRS, Université Lyon 1, 69622, Villeurbanne, France*
[2]*Laboratoire de Physique Moléculaire, Université de Franche-Comté, 25030, Bescançon, France*

(Received 23 February 2000)

A new mechanism for electron emission from planar cathodes is described. The theoretical analysis shows that, with an ultrathin wide band-gap semiconductor layer (UTSC) on a metal, the surface barrier is lowered to ~0.1 eV due to the creation of a space charge induced by the electrons injected from the metal. The barrier height depends mostly on the UTSC thickness and not on the state of the surface, as in thermionic and field emissions. This mechanism explains the measured stable emission at 300 K and 10^{-7} Torr, with a threshold field of only ~50 V/μm, from these solid-state field-controlled emitters.

PACS numbers: 79.70.+q, 85.30.De, 85.45.Bz, 85.45.Db

In conventional electron emission mechanisms, such as thermionic and field emission, to obtain emission current it is necessary to apply either high temperature (>1300 K) for electrons to overcome the work function or high field (>5000 V/μm) to narrow the tunneling barrier. In both cases, the surface barriers are fixed by the nature of the solid, the crystallography, and the adsorption state of the cathode surface. We have recently proposed the solid-state field-controlled emitter (SSE) as a paradigm shift for surface electron emission [1]. The basic structure of SSE is an ultrathin wide band-gap n-type semiconductor (UTSC) layer deposited on a metallic surface (Fig. 1). These cold cathodes emit stable electron currents with operating field F_{app} having a threshold value in the range of ~50 V/μm (2 orders of magnitude less than in field emission), in a poor vacuum environment (~10^{-7} Torr), and for different cathode geometries as plane, hairpin, or conical tip [1,2]. The main experimental results are (i) appearance of the emission current for a low threshold value of F_{app} without the need of a seasoning process, (ii) uniform and stable emission over the whole flat surface of the SSE, and (iii) emission characteristics that cannot be interpreted by the conventional thermionic or field emission mechanisms. Figure 2 is an example of the experimental current density J versus applied field F_{app} characteristics of SSE planar cathodes [3]. We have proposed a qualitative model to explain these results [4] in which the electron emission from the SSE cathodes results from a serial two-step mechanism: The first step is the injection of electrons at the solid-state Schottky junction from the metal into the UTSC medium, followed by a second step which is the electron emission from the UTSC surface that becomes, under the control of an applied field F_{app}, a surface with a low electron affinity (LEA situation for $\Delta\Phi_E \lessapprox 2$ eV) or with a negative electron affinity (NEA situation for $\Delta\Phi_E \lessapprox 0$) with $\Delta\Phi_E$ the potential difference between the metal Fermi level and the vacuum level. The injected charges induce a large band bending in the UTSC layer, with the consequence being a drastic lowering of the emission barrier $\Delta\Phi_E$, which can become low enough to allow emission of electrons through it or over it. As the standard Richardson and Fowler-Nordheim analysis familiar to thermionic and field emission calculations from metal or semiconductor surfaces is no longer applicable, as well as the recent approaches for carbon-film emission [5–7], the purpose of this study is to investigate the electron emission properties of the SSE by a rigorous numerical simulation analysis. The numerical implementation for SSE provides a flexible method to obtain the potential barriers that govern the emission current densities J. The analysis has been directed to answering three main questions: (i) What is the physical process that allows the electron emission from the UTSC and how can it be controlled by F_{app}? (ii) What is the variation of J vs F_{app}? (iii) What are the important parameters in the definition of the SSE concept? We show below that the present calculations can satisfactorily explain the experimental results.

The model consists of (i) a basic SSE structure with an UTSC layer in the range of 2 to 10 nm thick [TiO_2, for example, with $\epsilon = 35$; electron affinity = 4.5 eV; band gap = 3 eV; and a doping level at −0.2 eV under

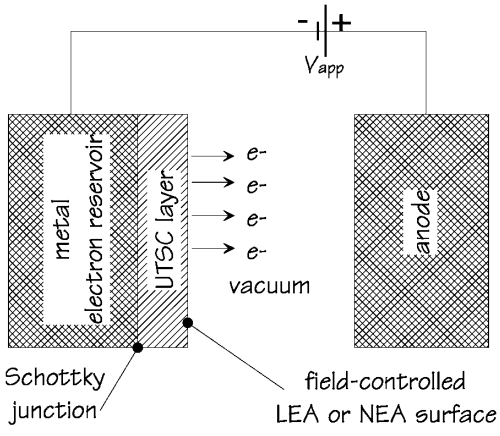

FIG. 1. Schematic representation of a SSE structure.

 0031-9007/00/85(4)/864(4)$15.00

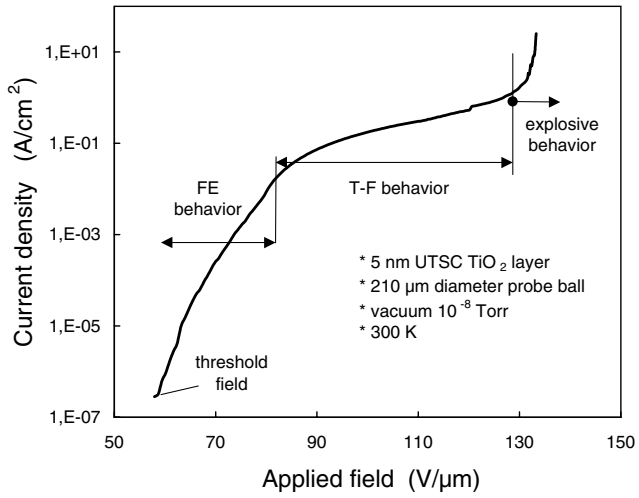

FIG. 2. Experimental current density J vs applied field F_{app}, characteristics of a SSE. Electron optics numerical simulation was used to obtain J and F_{app} from the measured total current I and applied voltage V from a flat SSE [3].

the conduction band (CB)], deposited on a metallic surface (Pt, for example, with Fermi level at 9.45 eV and work function = 5.3 eV), (ii) a Schottky junction between the metal and the UTSC with the conventional energy band relation [8], (iii) a triangular representation of the vacuum barrier including the image potential at the surface of the semiconductor, (iv) a numerical integration of the Poisson's equation to evaluate the equilibrium space charge distribution Q_{sc} inside the UTSC, and (v) a calculation of J by the resolution of the one-body Schrödinger equation using a Green's formalism based on the numerical resolution of the self-consistent Lippmann-Schwinger (LS) equation [9]. The calculations are one dimensional, as confirmed by experimental measurements showing a very uniform emission over the whole SSE flat surface [3]; and the charge densities for electrons in the CB, as well as for holes in the valence band, are assumed to be given by the Fermi-Dirac statistics. The boundary conditions are (i) at equilibrium and at the Schottky interface, the two Fermi levels are accorded; (ii) the field at the UTSC surface with vacuum is $F_{\mathrm{app}}/\epsilon$, with ϵ the dielectric constant.

Q_{sc} is given by the resolution of the Poisson's equation

$$\frac{d^2V(z)}{dz^2} = \frac{e^2}{\epsilon}[n(z) - n_0 - p(z) + p_0], \qquad (1)$$

within a quasiequilibrium condition, which means within a zero emission current approximation (ZECA) [$n(z)$ is the conduction electronic density, $p(z)$ is the hole density, and n_0 and p_0 are the intrinsic carrier densities of n and p, respectively [8]]. This implicitly assumes that the electrons are in thermal equilibrium among themselves and ZECA is valid as long as J is small relative to the electron supply function [10]. The potential distribution $V(z)$ is calculated by starting from the metallic boundary with an initial value corresponding to the Schottky barrier height and propagating it by using a finite differences method based on the second order series development

$$V(z + h) = V(z) + h\frac{dV}{dz} + \frac{h^2}{2}\frac{d^2V}{dz^2}, \qquad (2)$$

until the UTSC surface with vacuum, where dV/dz is the field inside the UTSC [11] and h is the discretization step. The propagation is done by modifying the polarization of the UTSC in an iterative process until the field at its surface reaches $F_{\mathrm{app}}/\epsilon$.

The quantum transport through this one-dimensional potential barrier is analyzed using a transmission coefficient, $T(E)$, approach [12]. The current density between the electron reservoir (metal) and the vacuum through the UTSC layer is given by [13]

$$J = \frac{me}{4\pi^2\hbar^3}k_BT\int dE\,T(E)\ln(1 + e^{(E_F-E)/k_BT}), \qquad (3)$$

where m is the mass of electron, k_B is the Boltzmann constant, T is the temperature, E_F is the Fermi level in the metal, and E is the energy of the electron. $T(E)$ is numerically calculated by means of the LS self-consistent equation which allows us to introduce in a reference system, having analytical solutions, a perturbation corresponding to the UTSC layer [14,15]. The reference system corresponds to the one-dimensional system constituted by a metal-metal polarized junction. The LS equation is

$$\psi(z) = \psi_0(z) + \int dz\,G_0(z, z'; E)V(z)\psi(z), \qquad (4)$$

where ψ is the wave function of the electron in the whole system, ψ_0 and $G_0(z, z'; E)$ are the wave function and the Green's function of the reference system, respectively. The solutions of the corresponding one-body Schrödinger equation are expressed by means of Airy functions.

The main results are as follows:

(1) The potential distribution across the system.—The resolution of the Poisson's equation gives two solutions corresponding, respectively, to the energy band diagrams 0 and 1 of Fig. 3. The first solution corresponds to a system with a very small value of Q_{sc}, which is very close to the initial Q_{sc} at the formation of the Schottky junction with the small band bending at the UTSC surface due to the presence of F_{app}. The second solution is obtained when a large value of Q_{sc} populated the CB of the UTSC and leads to an important band bending inside this layer which is illustrated by the evolution of diagram 0 towards 1 in step 1 of Fig. 3. The formation of Q_{sc} results from an electronic injection, through the reverse bias Schottky junction, from the metal into the CB of the UTSC by a thermionic mechanism and a tunneling process. The tunneling is either resonant through the donor states located near the CB bottom or direct when the band bending becomes sufficient. This implies that the injection starts for a threshold value of F_{app} and stops when the second equilibrium state is reached. The main result is that, at the second equilibrium state, $\Delta\Phi_E$ is only in the range of a few tenths of eV.

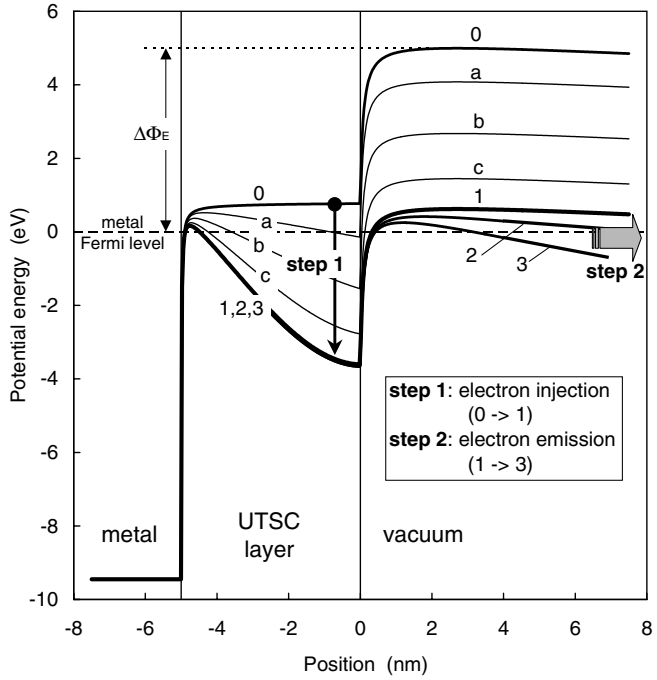

FIG. 3. Evolution of the energy band diagram of a SSE during the serial two-step mechanism. Step 1 is the electron injection from the metal into the UTSC with $F_{app} = 50\ V/\mu m$. The consequence is a drastic lowering of $\Delta\Phi_E$ (diagrams 0, a, b, c, and 1 are for $Q_{sc} = +1.8 \times 10^{-6} e\ nm^{-2}$, $-1.8 \times 10^{-3} e\ nm^{-2}$, $-0.4e\ nm^{-2}$, $-1.3e\ nm^{-2}$, and $-2.2e\ nm^{-2}$, respectively). Step 2 is the electron emission, from the UTSC surface, through and over the distorted emission barrier by increasing F_{app} (50 $V/\mu m$, 100 $V/\mu m$, and 140 $V/\mu m$, respectively, for diagrams 1, 2, and 3).

(2) The emission current versus the applied field.—From this second equilibrium state, if F_{app} is increased the potential distribution inside the UTSC layer stays practically unmodified; only the vacuum barrier is distorted as shown by diagrams 1 to 3 of step 2 in Fig. 3. The consequence is a lowering of $\Delta\Phi_E$ and a narrowing of the tunneling barrier. Such a modification of the emission barrier means that the emission current increases by increasing F_{app} from a threshold value. The theoretical variation of J vs F_{app} is very similar to the experimental plot of Fig. 2, and the emitted electrons have a characteristic energy dispersion plotted in Fig. 4. This spectrum, with the concomitant presence of the lower and upper energy tails, shows that the contribution of electrons passing over the barrier is no more negligible compared to the tunneling electrons. It is very similar to the energy distribution spectra obtained from high temperature T-F emission from metal surfaces [16]. However, when F_{app} reaches values that the lowering of the barrier develops a NEA behavior, an "explosive" increase of J will occur.

(3) The band bending versus the UTSC layer thickness.—The main parameter that allows the understanding of the emission behavior of the SSE is the important band bending, ~5 eV. If F_{app} is necessary to inject the electrons from the metallic reservoir, it does not determine the large band bending observed inside the UTSC layer. This band bending is related to the large values of Q_{sc} that can be injected into the UTSC layer, as shown in Fig. 3. Q_{sc} values are an inverse function of the layer thickness, and Fig. 5(a) is an illustration of this behavior. Consequently, as shown in Fig. 5(b), the lowering of $\Delta\Phi_E$ until LEA behavior can be obtained only for thicknesses of the UTSC layer smaller than 6 or 7 nm. This last value defines then the upper limit of the UTSC thickness for SSE operation. On the other side, the lower limit of the thickness is determined by the requirement to keep Q_{sc} inside the UTSC layer. This lower limit for SSE operation is then given by

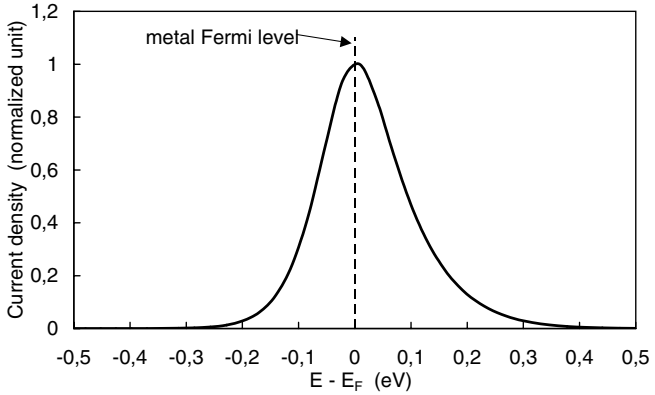

FIG. 4. Energy dispersion spectrum of the emitted electrons from a SSE ($T = 300$ K; $F_{app} = 140\ V/\mu m$).

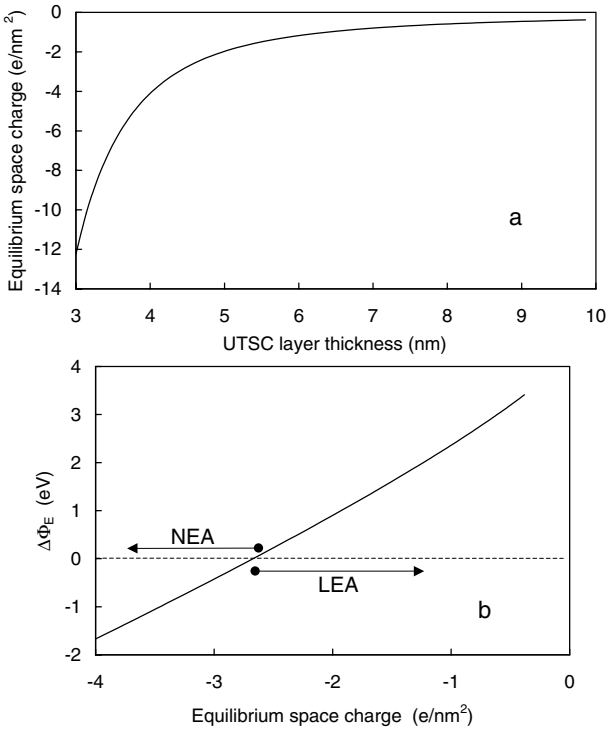

FIG. 5. (a) Variation of the equilibrium space charges versus the thickness of the UTSC layer. (b) Variation of the emission barrier height in function of Q_{sc}.

the appearance of the NEA behavior, i.e., for a thickness ~4 nm, because therefore no significant increase in the concentration of electrons in the CB can happen.

Modifying the materials will change the numerical values of the results, in particular, J vs F_{app}, but not the general behavior. Minor discrepancies between experimental results and theoretical predictions can therefore be due to the fact that the correct values of the materials used in the experiments are not known with precision, in particular, the exact value of the donor level which is related to the presence of impurities and defects. In addition, the exact values for the upper and lower limits for the thickness of the UTSC for SSE operation will change depending on the UTSC layer properties; however, the thicknesses should remain in the range of 3 to 7 nm. A more complete analysis and comparison between experimental measurements and theoretical predictions will be done [17].

In conclusion, we have shown experimentally and theoretically that electrons are emitted from a cathode having its emission barrier controlled by the space charge created inside a deposited UTSC layer. Stable currents are obtained at room temperature, in poor vacuum environment, and with operating fields 2 to 3 orders of magnitude less than for field emission. This alternative mechanism alleviates the constraints intrinsic to thermionic and field emissions. The SSE not only introduces a new concept for electron emission but meets most of the requirements for the development of vacuum microelectronics devices and large area cold cathodes, for flat-panel displays, for example.

We acknowledge the support of Hewlett-Packard Co. (Palo Alto, CA) for this research. Discussions with J. P. Dupin, D. Guillot, and V. Semet are greatly appreciated.

*Corresponding author.
Email address: vuthien@dpm.univ-lyon1.fr

[1] Vu Thien Binh, J. P. Dupin, and P. Thevenard, Université Lyon 1 patent pending No. 99 06 254 (1999).
[2] J. C. Plenet and Vu Thien Binh, Université Lyon 1 patent pending No. 99 14 474 (1999).
[3] Vu Thien Binh *et al.,* in Proceedings of the Spring–Materials Research Society Meeting, San Francisco, 2000 (to be published).
[4] Vu Thien Binh *et al.,* J. Vac. Sci. Technol. B **18**, 956 (2000).
[5] M. W. Geis *et al.,* Nature (London) **393**, 431 (1998).
[6] P. H. Cutler, N. M. Miskovsky, P. B. Lerner, and M. S. Chung, Appl. Surf. Sci. **146**, 126 (1999).
[7] K. A. Dean and B. R. Chalamala, Appl. Phys. Lett. **76**, 375 (2000).
[8] S. M. Sze, *Physics of Semiconductor Devices* (Wiley Interscience, New York, 1981).
[9] Ch. Adessi and M. Devel, Ultramicroscopy (to be published).
[10] K. L. Jensen and A. K. Ganguly, J. Vac. Sci. Technol. B **12**, 770 (1994).
[11] K. L. Jensen, J. Vac. Sci. Technol. B **11**, 371 (1993).
[12] A comparison between the different methods is given by K. L. Jensen and A. K. Ganduly, J. Appl. Phys. **73**, 4409 (1993).
[13] C. B. Duke, *Tunneling in Solids* (Academic Press, New York, 1969).
[14] N. D. Lang and A. R. Williams, Phys. Rev. B **18**, 616 (1978).
[15] A. A. Lucas *et al.,* Phys. Rev. B **37**, 10 708 (1988).
[16] L. W. Swanson and A. E. Bell, in *Advances in Electronics and Electron Physics,* edited by L. Marton (Academic Press, New York, 1973), Vol. 32, p. 193.
[17] Vu Thien Binh, J. P. Dupin, Ch. Adessi, and V. Semet (to be published).